COMPASS : A DESIGN TOOL FOR HIGH-POWER SEMICONDUCTOR DEVICES

C. Christiaan Abbas

Brown Boveri Research Center, CH-5405 Baden, Switzerland

SUMMARY

Most of the present computer programs for the simulation of semiconductor devices have been designed for the analysis of the devices used in integrated circuits. However, such simulations are now increasingly important also for power semiconductor devices, which switch large currents (up to 2 kA) and voltages (up to 5 kV). In the present report a new transient one-dimensional computer program called COMPASS (COMputer Program for the Analysis of SemiconductorS) designed for the simulation of bipolar semiconductor devices, especially high power devices, is presented. COMPASS calculates the switching behaviour of a semiconductor device embedded in a circuit consisting of an inductive load and a snubber circuit, the only input parameters being the structure of the device, the profile of the carrier-lifetimes, and the parameters of the circuit. COMPASS takes into account the Shockley-Read-Hall and Auger recombination processes, the lattice, ionized impurity, and carrier-carrier scattering, the saturation of the carrier-velocity at high electric fields, and impact ionization. The performance of COMPASS is illustrated by comparing measured and calculated data, and by showing how the application of COMPASS can lead to power semiconductor devices with optimized transient behaviour.

1. INTRODUCTION

In the case of power semiconductor devices many interesting phenomena, like the turn-off process of diodes or thyristors, can be accurately described by one-dimensional models. The advantage of computer programs for one-dimensional models, as compared with ones for two- and three-dimensional models, is that they require less CPU time and computer memory. Therefore, a reliable, transient one-dimensional simulator like COMPASS [1] is an adequate tool to investigate the processes taking place in bipolar semiconductor

structures and to speed up the development process of new or improved power semiconductor devices.

Fig. 1 shows the basic structure of COMPASS. The input data used by COMPASS are generated by an interactive input processor, INCOMP, and the results of a simulation can be plotted by the output processor, PLCOMP.

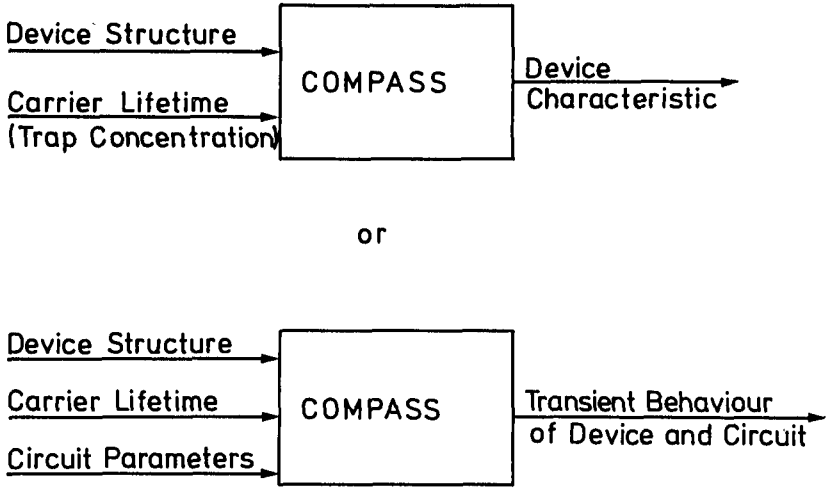

Fig. 1. Basic structure of COMPASS.

COMPASS, which is entirely written in FORTRAN-77, is now running on the following computers : VAX 11/750, VAX 11/780, VAX 8600, and HP 9000 series 500.

After a brief description of COMPASS in section 2, a simulated turn-off process of a diode is compared with measured data in section 3. In section 4, it is shown how an axial varying carrier-lifetime profile can be used to improve the trade-off between the forward characteristic and the turn-off behaviour of a power diode.

2. COMPASS

In [1] a detailed description of COMPASS is given. In this section the main features of COMPASS are presented.

2.1. Numerics

In COMPASS each simulation starts with the calculation of the equilibrium condition, because the distribution of the independent variables, which are the electrostatic potential and the electron and hole concentrations can be well esti-

mated analytically for this condition. Subsequently, the steady-state and transient simulations are performed.

The electron and hole continuity equations and the Poisson equation, are solved simultaneously by Newton's method. The partial derivatives of the semiconductor equations with respect to the independent variables, which are needed for the determination of the elements of the Jacobian matrix, are analytically calculated. The first and second derivatives with respect to x are calculated by the usual two and three point finite difference equations.

The Gaussian elimination process is divided into two steps. The triangular decomposition of the Jacobian matrix is done by the DGBFA subroutine of LINPACK [2] and the back and forward substitutions by the DGBSL subroutine of the same package. In order to save CPU time, the calculation of the elements of the Jacobian and its triangular decomposition are skipped, when the iteration process is close to convergence. Then the stored decomposed Jacobian is used for the forward and the backward substitutions.

The distribution of the grid points is not equidistant, but adapted to the device structure as defined by the profile of the impurity concentration. However, the distribution of the grid points is not adapted to the actual state of the device but constant as a function of the time. The smallest distances between the grid points occur near the p-n junctions, i.e. at the largest gradients of the impurity concentration.

At the contacts the usual equilibrium and zero space charge boundary conditions are assumed. Since COMPASS is a voltage driven program, the electrostatic potential at the contacts is either explicitly defined (simulations of the steady-state), or defined by the interaction between the circuit and the semiconductor device (transient simulations).

For the calculation of the electron and hole currents the well-known Scharfetter-Gummel equations are used [3]. It should be noted, that these equations have one major disadvantage: the calculation of small currents in highly doped regions is not exact [1]. Equation (1) shows the Scharfetter-Gummel expression for the electron current density, j_n, at a grid point h in the middle between the grid points i and i+1:

$$(1)\quad j_{n_h} = e\,\mu_{n_h}\,\frac{U_T}{\Delta x}\,\{\,B(z)\,n_{i+1} - B(-z)\,n_i\,\}\,.$$

In this equation e is the magnitude of electronic charge, μ_n ist the electron mobility, U_T is the thermal voltage kT/e, Δx is the distance between the grid points i and i+1, $n_{i,i+1}$ are the electron concentrations at the grid points i and i+1, and B(z) is the Bernoulli function of $z = (\psi_{i+1} - \psi_i)/U_T$:

$$(2) \quad B(z) = \frac{z}{e^z - 1}$$

Equation (1), which is used in COMPASS, clearly indicates where the mentioned problem originates. Assuming a highly doped cathode region, the electron concentration is large, e.g. 10^{20} cm^{-3}. If the device is blocking, the current density may be 10^{-6} A/cm^2. Assuming that $(e\ \mu_n\ U_T/\Delta x) = 8.3\ 10^{-14}$ Acm, then $B(z)\ n_{i+1} - B(-z)\ n_i = 1.2\ 10^7$ cm^{-3}. This value results from the substraction of two numbers of the order of n_{i+1}, since $B(\pm z)$ is almost equal to one for small values of z. Therefore, and because double precision numbers have about 16 significant digits, the difference $B(z)\ n_{i+1} - B(-z)\ n_i$ has only <u>three</u> significant digits. In another part of the device, where the electron concentration is 10^7 times smaller, but where the same current flows, there will be <u>ten</u> significant digits.

A solution to this problem, that the exactness of the calculation of the current densities depends upon the value of the electron (or hole) concentration, has not been found yet. In COMPASS the consequence of this problem is that, if the currents are very small, the value of the current calculated in the heavily doped regions oscillates around the more exact value of the current calculated in the weakly doped part of the device.

In the transient case the pure implicit formulation of the discretised time-dependent equations is used, because, as has been shown in [1], the Crank-Nicolson formulation is only stable for certain combinations of the grid point distribution and the time steps Δt.

2.2. Physics

COMPASS has two modes for the calculation of the Shockley-Read-Hall recombination rate. It is either possible to use the single energy level equation [4,5], or to take into account both energy levels related to gold in silicon for gold doped devices [6]. For the calculation of the Auger recombination rate the Auger coefficients of Dziewior and Schmid are used [7].

For the calculation of the carrier-mobility as a function of the lattice, ionized impurity, and carrier-carrier scattering, μ_{licc}, the equations compiled by Dorkel and Leturcq [8] are used. In COMPASS the saturation of the carrier-velocities at high electric fields is taken into account by using the equation derived by Thornber [9]. In COMPASS the following equation is used to calculate the resulting effective mobility μ [1] :

$$(3)\quad \mu = \mu_{licc} \left\{1 + \left(\frac{\mu_{licc} F}{v_c}\right)^2 \left(\frac{\mu_{licc} F}{v_c} + g\right)^{-1} + \left(\frac{\mu_{licc} F}{v_s}\right)^2 \right\}^{-1/2}.$$

In equation (3), v_c and v_s are the critical and saturation velocities of either the electrons or the holes, g is a fit parameter, and F is the electric field.

For the calculation of the ionization rates, COMPASS also uses an equation derived by Thornber [10], which is compatible with the data measured by van Overstraeten and de Man [11].

3. COMPARISON OF THEORY AND EXPERIMENT

An important aspect of numerical analysis is to ensure that the results from the simulations compare well with the data obtained from measurements. Fig. 2 shows the profile of the impurity concentration of a p-i-n Diode measured with the Spreading Resistance technique. The area of the device is 16 cm^2.

Fig. 3 shows the calculated turn-off behaviour of this diode embedded in the circuit shown in Fig. 4.

It should be noted especially that the value of the carrier-lifetime is an optically measured value. Thus only measured data are used as input for COMPASS. As can be seen from Fig. 3 the agreement between the data calculated by COMPASS and the measured data is very good.

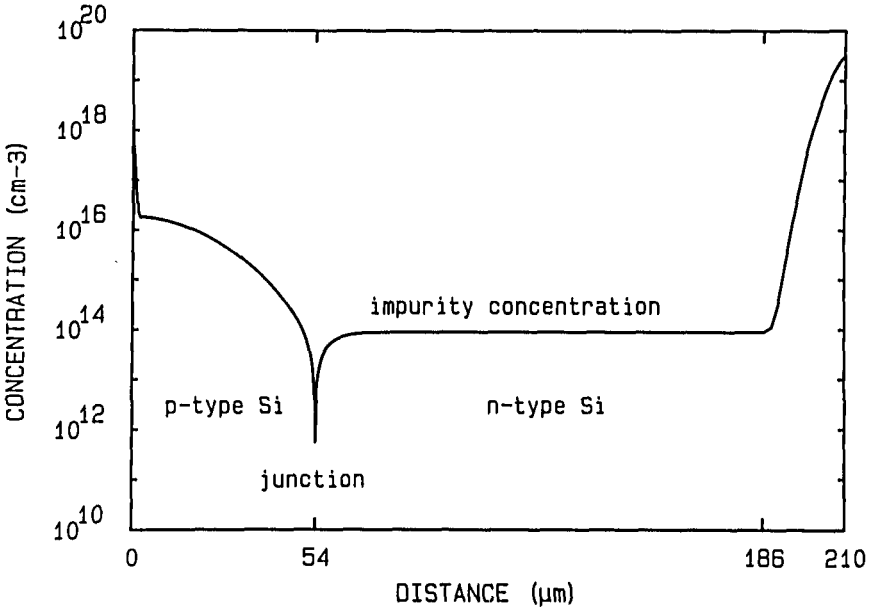

Fig. 2. Measured profile of the impurity concentration in a power Diode.

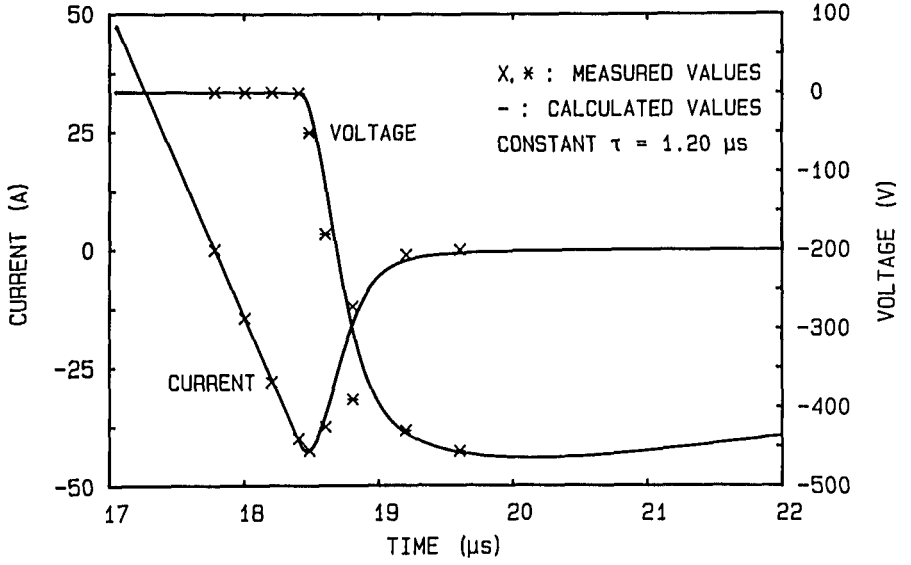

Fig. 3. Comparison of the measured and the calculated current and voltage during a turn-off process of the diode shown in Fig. 2; T=300 K, I_F= 1160 A, V_A=-380 V, L=5.84 µH, R_{snub}= 6.8 Ω, and C_{snub} = 0.47 µF.

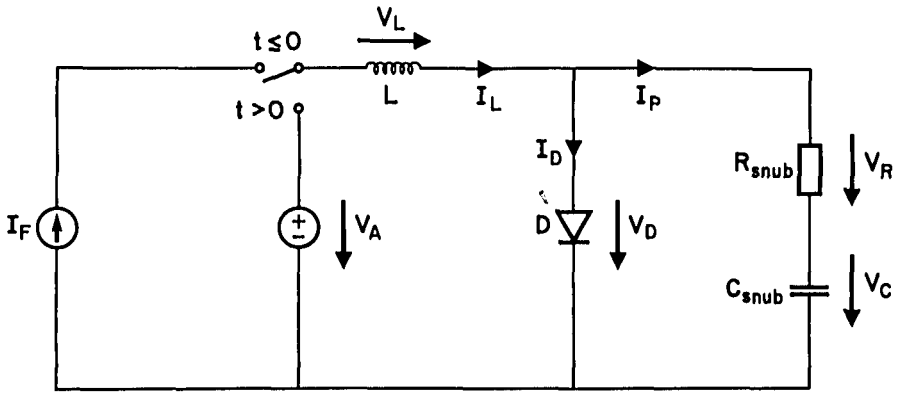

Fig. 4. Circuit which is taken into account in COMPASS for transient simulations.

It is shown in [1] that the best correspondence between the calculated and the measured forward characteristic of this diode is obtained if the value of the high-injection carrier-lifetime is 1.04 μs. A possible explanation for this discrepancy between the values of the carrier-lifetime in the steady-state and transient simulations is that the distribution of the gold traps in the diode is not constant but a function of x. A possible profile which gives good agreement between measured and calculated data for both the forward and turn-off characteristics is shown in [1].

4. CARRIER-LIFETIME PROFILES FOR POWER DIODES

In [12] Adler and Temple present a detailed analysis of high-power rectifiers. However, considering the carrier-lifetime, they only investigate the influence on the diode behaviour of lifetime-control by means of electron irradiation or gold or platinum diffusion. All these ways of controlling the lifetime lead to a more or less homogeneous carrier-lifetime. In [13] Temple and Holroyd investigate the influence of carrier-lifetime profiles on the electrical characteristics of diodes and thyristors. However, they are mainly interested in optimizing the trade-off between the turn-off time and the forward characteristic of a device.

In addition to these investigations, Abbas discusses in [1] the influence of various structural parameters on the diode characteristics. In [1] the emphasis is not put on the turn-off time but on the reverse current and reverse voltage peaks. Here, an extension to this analysis is presented by investigating the influence of carrier-lifetime profiles on these turn-off parameters.

COMPASS allows for three different carrier-lifetime profiles in addition to a constant lifetime. These three profiles are a) a linear profile, in this case the lifetime linearly increases or decreases from the anode to the cathode, b) a steplike profile, in this case the lifetime jumps from one value to another one at some given x-coordinate, and c) a pulse shaped profile. Fig. 5 shows an example of such a pulse shaped profile of the trap concentration N_T. In COMPASS the relationship between the high-injection carrier-lifetime and the trap concentration is $\tau_{hi}=3.3\ 10^{7}/N_T$ s. In Fig. 5 τ_{hi} is 2.23 µs from the anode to x=60 µm, 0.1 µs from 60-80 µm, and 2.23 µs again from 80 µm to the cathode.

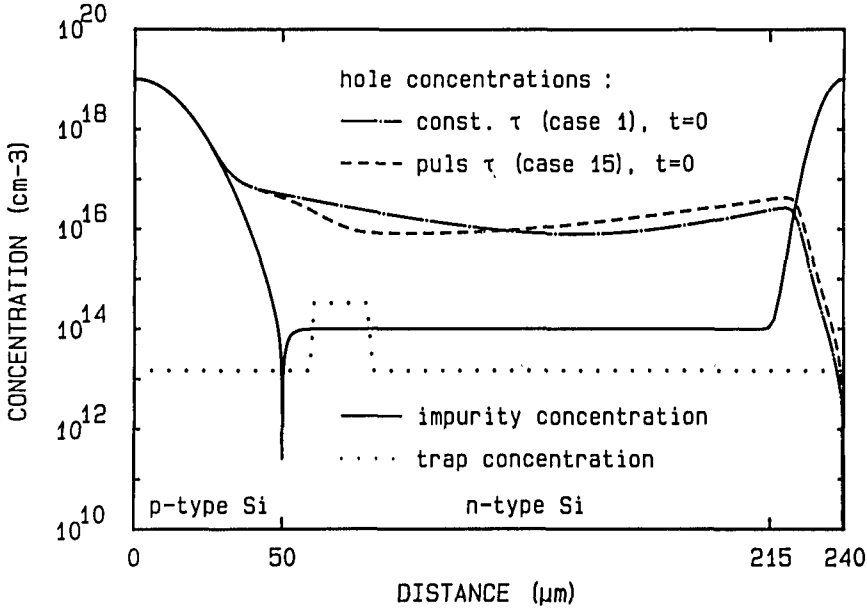

Fig. 5. Comparison of the distributions of the hole concentrations in the diode with the constant trap concentration (broken and dotted line) and in the diode with the indicated pulse shaped trap concentration profile (broken line).

A steplike profile is assumed to be an approximation to the diffusion profile of a slow diffusing trap, a pulse shaped profile to the profile of the trap concentration after proton irradiation. A linear lifetime profile does not directly have a physical meaning, however, it might still approximate the real lifetime profile in an actual device better than a constant lifetime.

Table 1 lists all the parameters which are identical for all the seventeen simulations of the devices with the different carrier-lifetime profiles presented in Table 2. As can be observed from Table 1, the lifetime profiles are chosen in

Table 1

Constant Data for all Simulations

	Value	Unit	Remarks
Thickness of the device	240	μm	
p-n junction depth	50	μm	
Impurity Concentration in the substrate	10^{14}	cm^{-3}	
Breakdown Voltage	1535	V	
Area of the Device	16	cm^2	
Forward Voltage Drop at 1200 A	1.226	V	(±1.3 %)
Starting Current, I_F	1200	A	(75 A/cm^2)
Applied Voltage, V_A	-400	V	
Inductance, L	5	μH	
Snubber Resistance, R_{snub}	40	Ω	
Snubber Capacitance, C_{snub}	0.47	μF	
Temperature	300	K	

such a way that the forward voltage drop at 1200 A is always 1.226 V. Therefore, the optimization procedure is rather easy : the device with the turn-off behaviour which is best suited to a specific application is the best device. In fact, the forward characteristics not only match at 1200 A and 1.226 V, they are almost identical over the whole simulated current and voltage range, as can be seen from Fig. 6 for the cases 1 and 15. However, as is shown in Fig. 5, the distribution of the concentration of the holes (and of the electrons and the distribution of the electric field) are quite different in these two diodes.

In Table 2 the type of the profile of the carrier-lifetime (of the trap concentration) is given in column 2. The third column contains the lifetime values. In the case of a linear lifetime profile the first value indicates the carrier-lifetime at the anode and the second one at the cathode of the diode. In the case of a steplike profile, the first value is the carrier-lifetime at the anode side of the device and the second one at the cathode side. The value in the third column is the x-coordinate at which the step in the lifetime occurs.

In the case of a pulse shaped lifetime profile, for an example see Fig. 5, the first value in column three is the carrier-lifetime in the low-lifetime region which extends from the first to the second value given in column four. The second value in column three is the carrier-lifetime in the rest of the device.

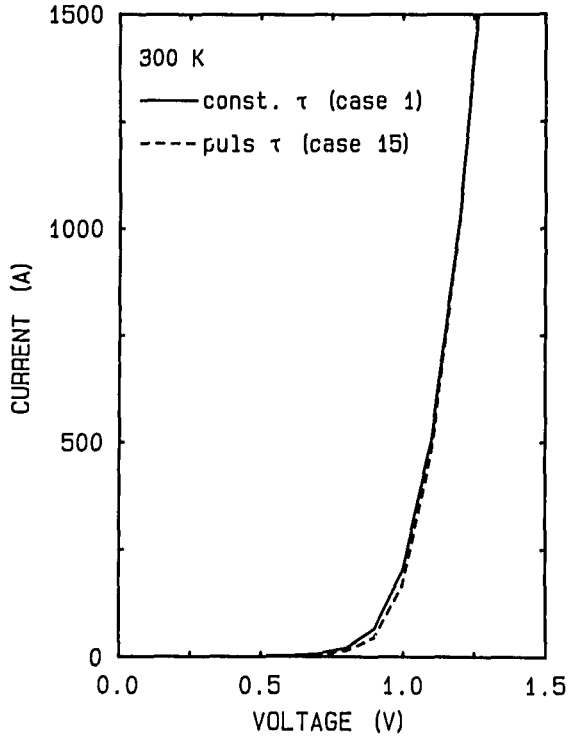

Fig. 6. Comparison of the forward characteristics of the diode with a constant trap concentration profile (solid line) and of the diode with the pulse shaped one (broken line).

Table 2

Carrier-Lifetime Profiles and Results

Case	Type	τ μs	x μm	$\hat{I}_r$ A	$\hat{V}_r$ V	t_{rr} μs	Q_{rr} μC
1	Constant	1		55.8	1367	1.08	37
2	Linear	0.5/4.3		42.0	806	1.16	30
3	Linear	12./0.5		81.8	1677	1.37	67
4	Steplike	0.5/1.1	50	51.5	1118	1.11	36
5	Steplike	0.5/1.1	100	39.9	744	1.30	33
6	Steplike	0.5/1.1	150	36.6	558	1.99	43
7	Steplike	1.3/0.5	190	70.0	1598	1.24	53
8	Steplike	2.0/0.5	140	94.6	1711	1.60	89
9	Steplike	500/0.5	90	154.7	1758	2.52	130
10	Pulse shaped	0.5/1.1	40-60	47.5	1039	1.06	32
11	Pulse shaped	0.1/2.4	40-60	48.0	754	1.62	49
12	Pulse shaped	0.5/1.1	50-70	48.4	1055	1.07	33
13	Pulse shaped	0.1/2.3	50-70	42.7	709	1.57	43
14	Pulse shaped	0.5/1.1	60-80	49.5	1085	1.08	33
15	Pulse shaped	0.1/2.2	60-80	39.3	684	1.52	38
16	Pulse shaped	0.5/1.1	70-90	51.0	1123	1.08	34
17	Pulse shaped	0.1/2.2	70-90	39.5	689	1.47	37

In Table 2 also the results of the simulations have been summarised, the fifth column contains the reverse current peak $\hat{I}_r$, the sixth one the reverse voltage peak $\hat{V}_r$, the seventh one the reverse recovery time t_{rr}, and the last one the reverse recovery charge Q_{rr}.

Within the scope of this paper, it is not possible to discuss each lifetime profile in detail. However, it is interesting to note that none of the devices with a lifetime profile is faster than the one with the constant lifetime. This is due to the fact that all devices have the same forward characteristic. It is also interesting to note that from a general point of view the linear lifetime profile No. 2 seems to be optimal. As compared with case 1, it reduces the reverse current peak by 25 %, the reverse voltage peak by 41 %, and the reverse recovery charge by 19 % while the reverse recovery time is only increased by 7 %.

In the case of the pulse shaped profiles it is obvious that the profiles with τ_{hi}=0.1 µs in the low-lifetime region lead to the more significant differences in the turn-off behaviour. On the other hand the profiles with τ_{hi}=0.5 µs in the low-lifetime region can be used to reduce the reverse voltage peak by at least 20 % without significantly changing any of the other turn-off parameters.

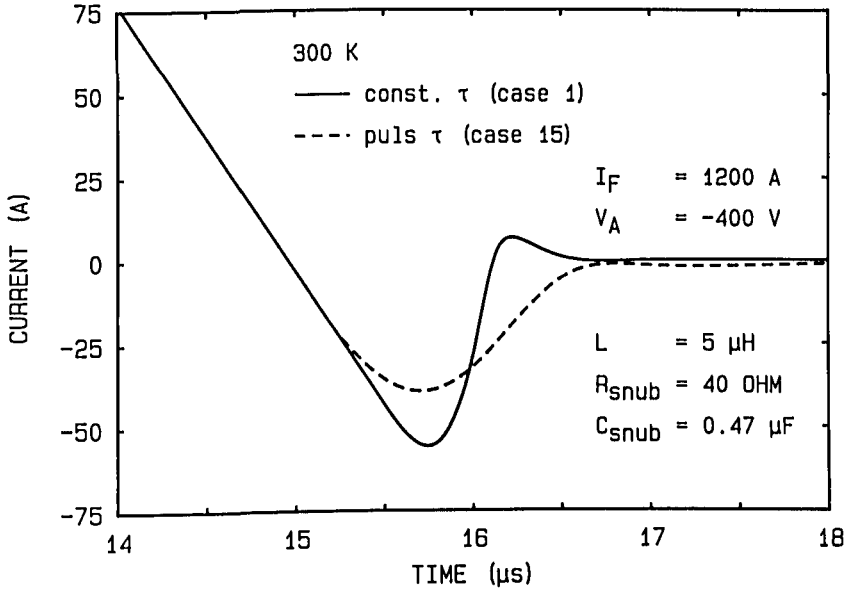

Fig. 7. Comparison of the reverse currents as a funtion of the time of the diode with the constant trap concentration (solid line) and of the diode with the pulse shaped trap concentration profile (broken line).

Now the main effects of a pulse shaped carrier-lifetime profile will be discussed in detail by comparing the differences in the turn-off behaviour of the diode with the constant lifetime, case 1, and the diode with the pulse shaped profile shown in Fig. 5, case 15.

In Fig. 5 the distribution of the hole concentration in diode 1 is compared with that in diode 15 for t=0, i.e. at the start of the transient simulation. This comparison shows that the low-lifetime region greatly modulates the carrier distributions. From Fig. 5 it can be expected that diode 15 has a smaller reverse current peak than diode 1, because the carrier concentration near the p-n junction is reduced.

It can further be expected that the reverse current of diode 15 slowlier decays after the reverse current peak, because more carriers are stored at the cathode side of the diode. Thus, diode 15 is expected to be a soft-recovery diode, or in terms of [12] diode 15 is less "snappy" than diode 1.

In Fig. 7 the reverse current during the turn-off process of diode 1 as a function of the time is compared with that of diode 15. As can be seen from Fig. 7 the differences between the reverse currents are as expected from Fig. 5.

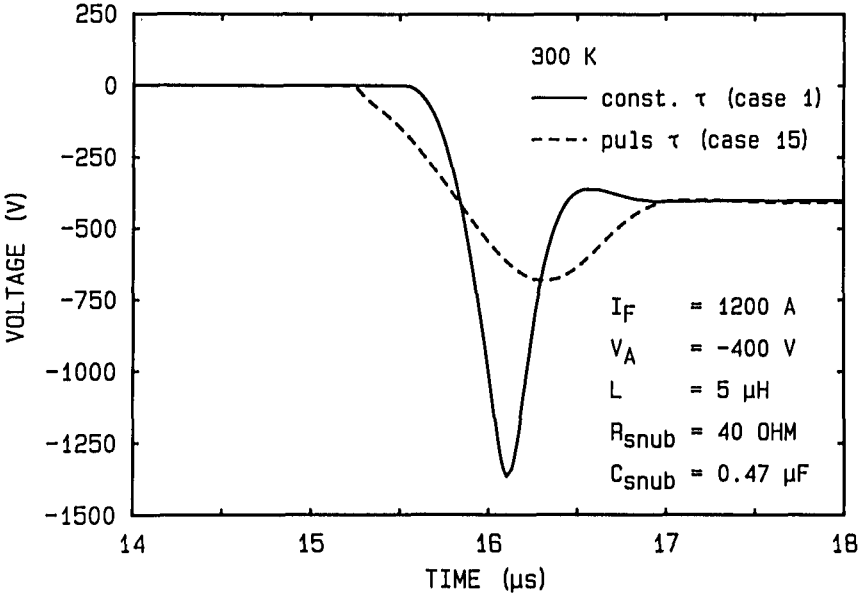

Fig. 8. Comparison of the reverse voltages as a funtion of the time of the diode with the constant trap concentration (solid line) and of the diode with the pulse shaped trap concentration profile (broken line).

From Fig. 7 it can be expected that due to the reduced gradient of the reverse current of diode 15 after its peak, the reverse voltage peak in the case of diode 15 is much smaller than that of diode 1. This is confirmed by Fig. 8.

As can be seen from Fig. 8, the differences between the reverse voltages as a function of the time of the diodes 1 and 15 are even more dramatic than the differences between the reverse currents. The reverse voltage peak of diode 15, $\hat{V}_r$=684 V, is only half as large as that of diode 1, $\hat{V}_r$= 1367 V. Fig. 8 shows that the reverse voltage peak is a good criterion to distinguish between hard- and soft-recovery diodes, provided that the diodes are tested in the same circuit.

Fig. 8 also shows that the reverse voltage of diode 15 rises much earlier than that of diode 1. As has been shown in Fig. 5, the carrier concentrations near the p-n junction in diode 15 are reduced as compared with diode 1. Therefore, the reverse current needs a shorter time to deplete the p-n junction in diode 15. Fig. 9 compares the distribution of the hole concentration in diode 1 with that in diode 15 for t=15.5 µs. At this time the p-n junction in diode 15 is already completely depleted, while the weakly doped part of diode 1 is still filled with carriers.

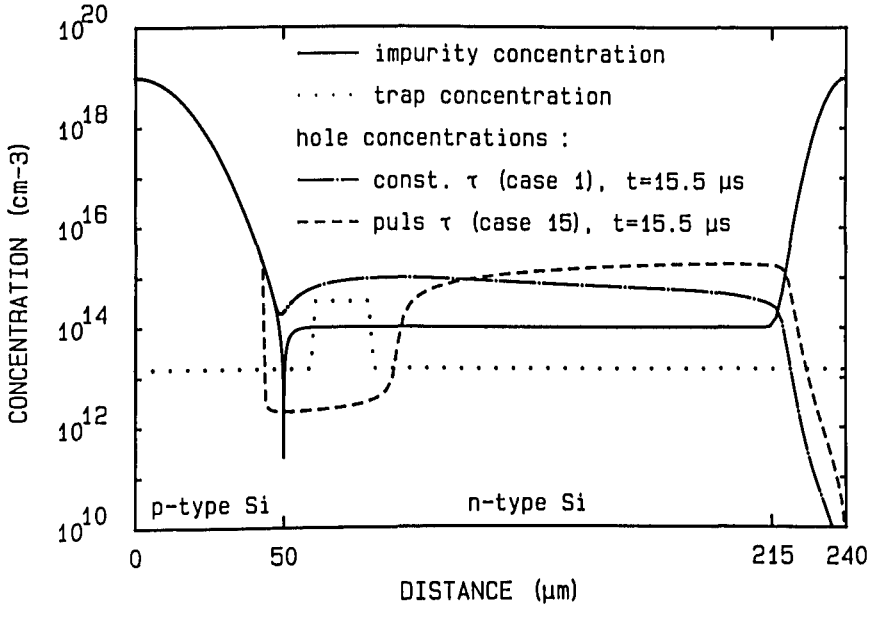

Fig. 9. Comparison of the distribution of the hole concentration at t=15.5 µs in the diode with the constant trap concentration (broken and dotted line) and in the diode with the pulse shaped trap concentration profile (broken line).

Fig. 9 also shows that the ratio between the hole concentration at the cathode side of diode 15 and that at the cathode side of diode 1 is now even larger than at t=0. This is due to both the longer lifetime at the cathode side of diode 15 and the smaller reverse current peak of diode 15, which leads to smaller carrier extraction by means of current flow. The additional carriers stored in diode 15 cause the slow reverse current decay after the reverse current peak shown in Fig. 7.

5. CONCLUSIONS

The comparison of experimental and calculated data shows that COMPASS accurately simulates the turn-off behaviour of power diodes.

Seventeen power diodes, each with a different carrier-lifetime profile, have been simulated. These lifetime profiles significantly influence the turn-off behaviour of the diodes, but they all lead to the same forward characteristic. It is shown that either low-lifetime regions extending from the anode surface to within the lowly doped base of the diode, or narrow low-lifetime peaks correlated with the junction depth result in optimum turn-off behaviour considering the reverse current and voltage peaks. The simulations show that "lifetime engineering" is a very effective method for optimizing the trade-off between the forward charateristic and the switching behaviour of a power diode.

It is also shown that by making full use of the possibility offered by COMPASS to look simultaneously at the electrical behaviour of a device and into that device, the differences between the electrical behaviour of different devices can be well understood.

ACKNOWLEDGMENTS

I would like to express my gratitude to my Ph.D. supervisors Prof. Melchior and Prof. Henrici of the Swiss Federal Institute of Technology, Zuerich, Switzerland, for their helpful and encouraging discussions during the origin of COMPASS. I would like to thank my colleagues in the power semiconductor device group of the Brown Boveri Research Center for their interesting discussions and Miss C. Laabs for her assistance in the preparation of the figures.

REFERENCES

[1] Abbas, C.C.
"Transient One-Dimensional Numerical Analysis of Bipolar Power Semiconductor Devices"
Ph.D. Thesis No. 7614, Swiss Federal Institute of Technology, Zürich, Switzerland, 1984.

[2] Dongarra, J.J. et al.
"LINPACK Users' Guide"
SIAM, Philadelphia, 1979.

[3] Scharfetter, D.L. and Gummel, H.K.
"Large-Signal Analysis of a Silicon Read Diode Oscillator"
IEEE Trans. on Electron Devices Vol. 16, p. 64, 1969.

[4] Hall, R.N.
"Electron-Hole Recombination in Germanium"
Phys. Rev. vol. 87, p. 387, 1952.

[5] Shockley, W. and Read, W.T.
"Statistics of the Recombinations of Holes and Electrons"
Phys. Rev. vol. 87, pp. 835-842, Sep 1952.

[6] Abbas, C.C.
"A Theoretical Explanation of the Carrier Lifetime as a Function of the Injection Level in Gold-Doped Silicon"
IEEE Trans. on Electron Devices vol. 31, p. 1428, 1984.

[7] Dziewior, J. and Schmid, W.
"Auger coefficients for highly doped and highly excited silicon"
Appl. Phys. Lett. vol. 31, pp. 346-348, Sep. 1977.

[8] Dorkel, J.M. and Leturcq, Ph.
"Carrier Mobilities in Silicon Semi-Empirically Related to Temperature, Doping, and Injection Level"
Solid-State Electronics Vol. 24, p. 821, Sep. 1981.

[9] Thornber, K.K.
"Relation of drift velocity to low-field mobility and high-field saturation velocity"
J. Appl. Phys. vol. 51, pp. 2127-2136, April 1980.

[10] Thornber, K.K.
"Applications of scaling to problems in high-field electronic transport"
J. Appl. Phys. vol. 52, pp. 279-290, Jan. 1981.

[11] van Overstraeten, R. and de Man, H.
"Measurements of the Ionization Rates in Diffused Silicon p-n Junctions"
Solid-State Electronics vol. 13, pp. 583-608, 1970.

[12] Adler, M.S. and Temple, V.A.K.
"Analysis and Design of High-Power Rectifiers", In: Semiconductor Devices for Power Conditioning (Ed. R. Sittig and P. Roggwiller), Plenum Press, New York, 1982

[13] Temple, V.A.K. and Holroyd, F.W.
"Optimizing Carrier Lifetime Profile for Improved Trade-off Between Turn-off Time and Forward Drop"
IEEE Trans. on Electron Devices Vol. 30, p. 782, 1983.